CONDENSED MATTER PHYSICS

Conference materials
UDC [621.793:621.315.5+544.164]::535.93::681.586
DOI: https://doi.org/10.18721/JPM.183.101

Comparison of the refractive index changes of nanolayers of amidated and carboxylated carbon nanotubes after adsorption of water and ammonia molecules

A.V. Romashkin [1] ✉, R.Yu. Rozanov [2], A.S. Vishnevskiy [3],
A.E. Mitrofanova [2, 4], A.N. Stebelkov [2], V.V. Nepomilueva [1],
D.D. Levin [2], V.V. Svetikov [2, 5], V.K. Nevolin [1]

[1] National Research University of Electronic Technology, Moscow, Russia;
[2] JSC "Zelenograd Nanotechnology Center", Moscow, Russia;
[3] MIREA – Russian Technological University, Moscow, Russia;
[4] Moscow Institute of Physics and Technology, Dolgoprudny, Russia;
[5] Prokhorov General Physics Institute of the RAS, Moscow, Russia
✉ romaleval@gmail.com

Abstract. Spray-deposited layers of amidated carbon nanotubes (ACNTs) were characterized using AFM, Raman scattering, and spectroscopic ellipsometry. The layer thickness, diameters, and band gap of ACNTs, as well as the changes in the refractive index (n) at 1319 nm and 1625 nm after H_2O and NH_3 adsorption in air and H_2O in N_2 were analyzed in comparison with carboxylated CNTs. Modeling the resonance peak shift due to changes in n for the ACNT-coated Si waveguide microring resonator after NH_3 adsorption allows us to propose the use of such a CNT layer set for integrated optical sensors for gas recognition tasks.

Keywords: carbon nanotube, ellipsometry, integrated optics, microring resonator, sensor

Funding: This research was supported by the Ministry of Science and Higher Education of the Russian Federation in the framework of state tasks FSMR-2023-0002 (spray deposition, post processing, AFM, Raman study, ACNT layers ellipsometry data analysis) and partially FSFZ-2023-0005 (RTU MIREA: ACNT layer ellipsometry in N_2 with H_2O, 2-propanol vapors).

Citation: Romashkin A.V., Rozanov R.Yu., Vishnevskiy A.S., Mitrofanova A.E., Stebelkov A.N., Nepomilueva V.V., Levin D.D., Svetikov V.V., Nevolin V.K., Comparison of the refractive index changes of nanolayers of amidated and carboxylated carbon nanotubes after adsorption of water and ammonia molecules, St. Petersburg State Polytechnical University Journal. Physics and Mathematics. 18 (3.1) (2025) 12–18. DOI: https://doi.org/10.18721/JPM.183.101

Материалы конференции
УДК [621.793:621.315.5+544.164]::535.93::681.586
DOI: https://doi.org/10.18721/JPM.183.101

Сравнение изменений показателя преломления нанослоев амидированных и карбоксилированных углеродных нанотрубок после адсорбции молекул воды и аммиака

А.В. Ромашкин [1] ✉, Р.Ю. Розанов [2], А.С. Вишневский [3],
А.Е. Митрофанова [2, 4], А.Н. Стебельков [2], В.В. Непомилуева [1],

Д.Д. Левин [2], В.В. Светиков [2, 5], В.К. Неволин [1]

[1] Национальный исследовательский университет «МИЭТ», Москва, Россия;

[2] АО «Зеленоградский нанотехнологический центр», Москва, Россия;

[3] МИРЭА – Российский технологический университет, Москва, Россия;

[4] Московский физико-технический институт (национальный исследовательский университет), г. Долгопрудный, Россия;

[5] Институт общей физики им. А. М. Прохорова РАН, Москва, Россия

✉ romaleval@gmail.com

Аннотация. Аэрозольно нанесенные слои амидированных углеродных нанотрубок (АУНТ) исследовались методами АСМ, комбинационного рассеяния света и спектроскопической эллипсометрии. Изменения показателя преломления (n) при 1319 нм и 1625 нм после адсорбции H_2O и NH_3 сравнивались с карбоксилированными УНТ. Смоделированный сдвиг резонансного пика Si микрокольцевого волноводного резонатора, покрытого АУНТ, при адсорбции NH_3 позволяет предложить использование таких слоев УНТ для интегрально-оптических сенсоров для задач распознавания газов.

Ключевые слова: углеродная нанотрубка, эллипсометрия, интегральная оптика, микрокольцевой резонатор, сенсор

Финансирование: Работа выполнена при поддержке Минобрнауки России в рамках государственного задания FSMR-2023-0002 (нанесение, постобработка, АСМ, КР спектроскопия, анализ эллипсометрии слоев АУНТ) и частично FSFZ 2023-0005 (РТУ МИРЭА: эллипсометрия слоев АУНТ в сухом N_2 с парами H_2O, 2-пропанола).

Ссылка при цитировании: Ромашкин А.В., Розанов Р.Ю., Вишневский А.С., Митрофанова А.Е., Стебельков А.Н., Непомилуева В.В., Левин Д.Д., Светиков В.В., Неволин В.К. Сравнение изменений показателя преломления нанослоев амидированных и карбоксилированных углеродных нанотрубок после адсорбции молекул H_2O и NH_3 // Научно-технические ведомости СПбГПУ. Физико-математические науки. 2025. Т. 18. № 3.1. С. 12–18. DOI: https://doi.org/10.18721/JPM.183.101

Introduction

For an integrated optical sensor array providing gas recognition, to achieve high sensitivity and form sensors with significantly different responses, it is important to develop thin modifying layers that significantly change the intrinsic refractive index (n) upon adsorption of the analyte [1–4]. Various modified carbon nanomaterials are promising for these tasks and can provide opposite sensor responses to the same analyte by changing only the functional group type [5] or by changing the carrier gas, which can alter their electronic structure [4, 6]. However, identifying the mechanisms of change in the n for CNTs functionalized by different groups at different wavelengths (λ) during the adsorption of various molecules remains a relevant task to develop such a sensor array. Previously, we studied the effect of molecular adsorption on the $n(\lambda)$ dependence only for carboxylated CNTs (CCNT) [4], but amidated CNTs (ACNT) have not been studied enough [5]. Therefore, the aims of this work are to study the change in the n after adsorption of NH_3 and H_2O in both air and oxygen-free (N_2) gas in order to identify the features of the sensor response of ACNT and its differences from CCNTs. Recent results on optical gas sensors based on microring resonators (MRR), which even use metallic layers (high extinction coefficient (k)), also open up new possibilities for the development of such sensor layers [7, 8].

Materials and Methods

We studied sparse and dense networks of ACNTs (P9-SWNT, Carbon Solutions). Layer thicknesses were measured by AFM (NT-MDT). The CNT diameter and band gap (E_g) were

evaluated [9] from the RBM-band Raman map (532 nm laser, Nano Scan Technology). ACNTs were spray deposited from a dispersion [4] onto an oxygen plasma treated Si substrate with 29 nm SiO_2. The residual solvent (ethanolamine, instead of N-methylpyrrolidone used for CCNT [4], due to the higher ACNT dispersion stability) was removed with iterative rinsing in solutions of acetic and then formic acid in butyl acetate. The ACNT layer absorbance was evaluated by the suppression of Raman of Si by the ACNT layer (at $\lambda \approx 550$ nm), and thickness was evaluated by AFM force–distance curves and lithography [4]. Conductivity type in air at a relative humidity (RH) of 40% was determined from the I–V characteristics for the ACNT sparse network on a SiO_2 (300 nm)/Si substrate. The resistive responses were measured by conductivity recovery after exposure for 15 min to ~12500 ppm H_2O (ΔRH ~45%) or 2-propanol (IPA) or ethanol (22% and 17% of saturated vapor at 23 °C, but both ~12500 ppm) or 2000 ppm NH_3 and compared with a denser ACNT network. The latter was also measured by spectroscopic ellipsometry (SENTECH Instruments) using similar analyte concentrations. It was performed at a 75° (70° in N_2) angle of incidence after exposure in a chamber with H_2O or NH_3 and after 25 min of desorption under normal conditions in the same sample area, but different for each analyte. Exposure to H_2O or IPA in N_2 was realized in situ [4]. The values of the n and k of the layer were estimated from the Drude–Lorentz model [4]. Numerical modeling (finite-difference time-domain and beam propagation methods, RSoft CAD) was performed to evaluate phase shift, losses, and resonance peak shift of the ACNT-coated Si waveguide and MRR after NH_3 adsorption at 1625 nm.

Results and Discussion

Dense and sparse ACNT networks (~10 nm and ~1 nm layers, Fig. 1, *a*) with diameters ranging from 1.3 to 1.7 nm (band gap $E_g \approx 0.63$–0.81 eV) show similar values for both CNT diameters, band gaps, and the dependence of absorbance on layer thickness compared to CCNTs [4] (Fig. 1, *b*). However, despite the similar (p-type) behavior of channel conductivity under gate field control [10] and similar ACNT resistive responses to H_2O and NH_3 (Fig. 1, *c*) compared to CCNT [11], the response to IPA (4%) is noticeably lower than to H_2O (40%) or even to ethanol (15%). For CCNT, on the contrary, the response to ethanol can be comparable to NH_3 in N_2 [12]. This can be used to form an array of resistive and optical sensors for gas recognition.

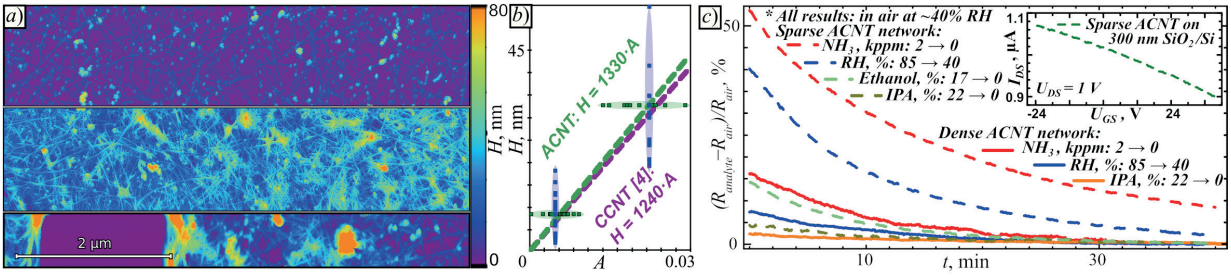

Fig. 1. AFM of sparse (top), dense (below) ACNT networks (*a*); graph of thickness versus absorbance (*b*); resistive response versus time after analyte exposure, inset: graph of current (I_{DS}) versus gate voltage (U_{GS}) (*c*)

When exposed to H_2O in air, the n of ACNT dropped slightly from 1.708 to 1.706 at 1625 nm ($\Delta n \approx -0.002$ as opposed to $\Delta n \approx 0.002$ for CCNT) and was 1.628, but did not change at 1319 nm ($\Delta n < 0.001$ versus $\Delta n \sim 0.012$ for CCNT, Fig. 2, *a*). The decrease in the n with increasing H_2O concentration occurs only near 1625 and 1410 nm (0.763 and 0.88 eV), which corresponds to the opposite changes in experimental $\Delta(E)$ and $\Psi(E)$ data for ACNT compared to CCNT (Fig. 2, *b*, *c*). This is presumably due to specific local changes in the density of states spectrum [13] for ACNTs. Although, when exposed to H_2O, near the main peak of $n(E)$, located at the photon energy close to the CNT band gap energy, an increase in the n is observed in air (but a decrease in N_2) with a slight decrease in the charge carriers concentration (p) for ACNTs in the Drude–Lorentz model: $\Delta p \approx -0.2\%$ in air, but $\Delta p \approx 1\%$ with RH change from 20 to 65% in N_2. This also corresponds to the resistive response in air for CCNT [11] and ACNT (~7% for dense network, Fig. 2, *c*). This effect is presumably related to a charge carrier type change: from holes in air to electrons in dry N_2, and is observed for both ACNT and CCNT [4, 6]. H_2O and NH_3 are donors for CNTs,

opposed to O_2 and NO_2, both of which are charge acceptors [13]. Thus, in air, H_2O and NH_3 reduce the concentration of CNT carriers [11], but in the absence of O_2, the opposite occurs for both ACNT and CCNT [4]. When exposed to NH_3, the n increased: from 1.697 to 1.710 at 1625 nm, from 1.620 to 1.638 at 1319 nm for ACNTs (Fig. 2, *a*). It corresponds to an increase in resistivity for both ACNTs (Fig. 1, *c*) and CCNTs [4, 11]. However, the ratio of responses to NH_3 and H_2O changes for ACNTs from −6.5 at 1625 nm to ~18 at 1319 nm. In contrast, for CCNTs this ratio is ~2 at 1625 nm and close to zero at 1319 nm. These changes in the ratio are apparently due to local but different changes in the band structure (and away from the edges of the CNT band gap) for both ACNT and CCNT and can provide the recognition of NH_3 versus H_2O in air using only CCNTs [4] or ACNTs, in contrast to resistive sensors [11].

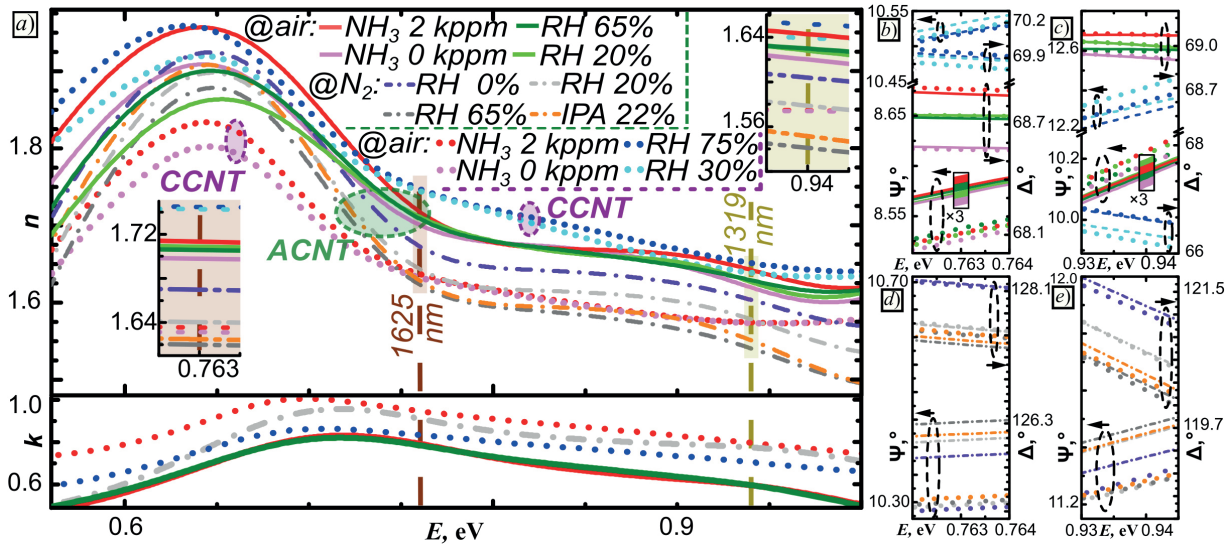

Fig. 2. n and k as a function of photon energy (E) for ACNT and CCNT (*a*), insets: enlarged $n(E)$ near λ = 1625 nm and λ = 1319 nm; Drude–Lorentz model (lines) for fitting to ellipsometry data (dots): $\Delta(E)$ and $\Psi(E)$ near the specified λ for the adsorption of H_2O and NH_3 in air (*b*, *c*); H_2O and IPA in N_2 (*d*, *e*)

The ACNTs, differing in the Δn direction in air after adsorption of NH_3 ("+" Δn) and H_2O (low, but "–" Δn) at 1625 nm with response (i.e., Δn) only to NH_3 at 1319 nm, also allow recognition of these gases. The response behavior differences for ACNT versus CCNT can only be associated with the different types of functional groups, since the remaining features of CNTs (E_g, the IR absorption peaks) are similar, and for non-functionalized CNTs, both NH_3 and H_2O are donors [4] and should not form the opposite sensor response in air. Although, H_2O in dry N_2 as a carrier gas gives a drop in the n for both ACNT and CCNT. The initial n value at λ = 1319 nm for ACNT in dry N_2 was 1.602. The n values during exposure to H_2O (subsequent N_2 purging) were at 20% and 65% RH: 1.579 (1.596) and 1.541 (1.565). The incomplete return is due to incomplete desorption during the 20-minute low-flow N_2 purge, which is typical for CNTs [4, 11]. For ACNT, despite the low resistive response to IPA in air and low Δn value at IPA exposure in N_2 near the main peak of $n(E)$ ($\Delta n \approx -0.02$ at $E \approx 0.65$ eV), the Δn was higher in modulus at 1625 nm and 1319 nm ($\Delta n \approx -0.05$), which is higher than for NH_3 in air. This indicates an improvement in the gas recognition capabilities when using several λ.

Modeling showed that the phase shift of 0.2° per 100 μm length is achieved in the Si waveguide coated with a 1 nm ACNT layer with a 50 nm SiO_2 sublayer. Thus, at ~22.5 mm a π/2 phase shift can be achieved. However, accounting for losses due to the high k of CNT obtained from ellipsometry (Fig. 2, *a*) does not allow the implementation of such an interferometer arm. The losses are ~0.9 dB per 100 μm (Fig. 3, *a*). The phase shift to loss ratio is 0.22°/dB.

Further increases in the sublayer do not lead to an improvement in this ratio. However, despite the high losses, the sensor structure can be implemented based on the ACNT-coated Si waveguide MRR structure (Fig. 3, *b*), similar to known results [7]. Modeling showed that

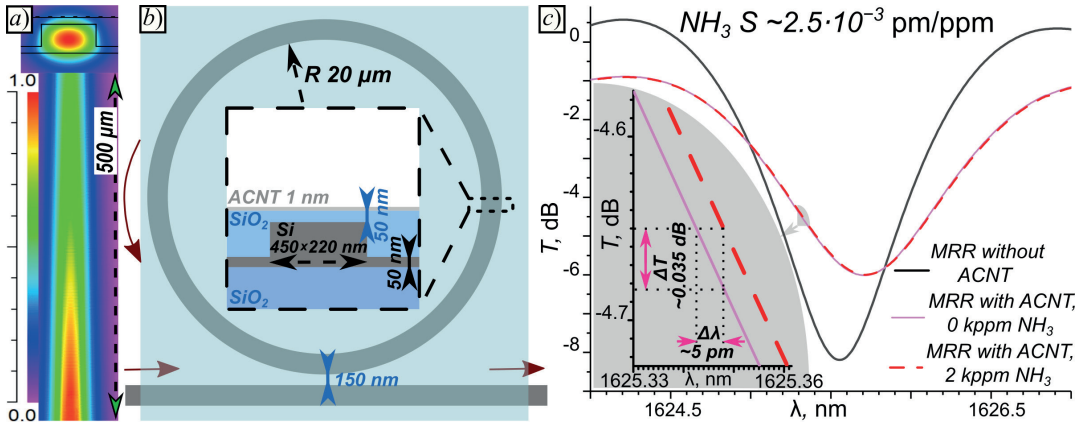

Fig. 3. Simulation results: electric field distribution and losses of ACNT-coated waveguide (*a*); scheme of microring resonator sensor (*b*); transmission spectra with resonance peak shift after NH_3 adsorption (*c*)

the quality factor (Q) of the proposed structure is 1900 without the CNT layer and 1200 with it, due to losses in the ACNT layer. Therefore, the MRR radius was chosen to be limited to 20 μm. The free spectral range was 6 nm, slightly higher than known [14] due to the use of a ribbed waveguide (Fig 3, *a*, *b*). Since the implementation of a gap between coupled waveguides less than 150 nm complicates the implementation [7, 8], this distance was chosen, even though critical coupling has not yet been fully realized. Thus, the extinction ratio and Q were lower than reported in the experiment [7]. The estimate of the resonance peak shift after NH_3 adsorption was about 5 pm (Fig. 3, *c*, red shift). This, assuming a noise level estimation of ~0.1 pm [7] and a linear response on concentration dependence, yielded an estimate of the sensitivity (S) to NH_3 as $2.5 \cdot 10^{-3}$ pm/ppm and a detection limit of ~40 ppm, comparable to the use of a special polymer, with higher changes in its n during the analyte adsorption [7]. However, recently a higher S value has been achieved for a similar sensor layer by changing only the MRR parameters [8]. Thus, it is presumed that the S of the proposed structure can also be improved. Moreover, the proposed structure with ACNT implemented for two λ can allow the recognition of NH_3 versus H_2O due to the difference in their response ratios at 1319 nm and 1625 nm. More reliable recognition can be implemented using ACNTs and CCNTs together, even at the same λ (even at 1625 nm), due to the larger differences in the responses between them. This is important because typically for a single sensor layer, the RH change can also affect the resonance peak shift, interfering with the analysis of target analyte [8]. However, changes in the band structure of CNTs during analyte adsorption can change not only the n but also k, which distinguishes them from the known polymer [7, 8], and can change the resonance peak width, complicating measurements.

Conclusion

Despite the similar behavior of the resistive response of ACNT and CCNT, ellipsometry showed significant changes in the ratio of responses to NH_3 and H_2O, expressed in the refractive index changes (Δn) at 1625 nm and 1319 nm for both ACNT and CCNT, especially between them, despite their differing only in the functional group types. Therefore, spray-deposited ACNTs or CCNTs can be used to modify the Si waveguide in a microring resonator (MRR) to manufacture the proposed integrated optical sensor, providing acceptable sensitivity, recognition of NH_3 versus H_2O. It can be implemented for two wavelengths using only ACNT or CCNT, or even for one wavelength when using ACNT and CCNT together in a sensor set capable of even better recognition of the gases. Despite the fairly high extinction coefficient of CNTs, the use of the MRR structure allows the use of such thin (~1 nm) CNT layers to implement integral optical sensor structures. The noticeable CNT Δn at photon energies far from the CNT band gap, presumably caused by the density of states changes in the CNT band structure with analyte adsorption, opens up new additional mechanisms for improving the sensors response selectivity. The combined use of such optical and resistive sensors significantly expands the possibilities of developing multisensor systems. This can be used for the development of integrated optical gas sensor array based on functionalized carbon nanomaterials and new principles of gas recognition.

REFERENCES

1. **Laplatine L., Fournier M., Gaignebet N., Hou Y., Mathey R., Herrier C., Liu J., Descloux D., Gautheron B., Livache T.,** Silicon photonic olfactory sensor based on an array of 64 biofunctionalized Mach-Zehnder interferometers, Optics Express. 30 (19) (2022) 33955.

2. **Huang G., Li Y., Chen C., Yue Z., Zhai W., Li M., Yang B.,** Hydrogen sulfide gas sensor based on titanium dioxide/amino-functionalized graphene quantum dots coated photonic crystal fiber, Journal of Physics D: Applied Physics. 53 (32) (2020) 325102.

3. **Huang X., Li X., Yang J., Tao C., Guo X., Bao H., Yin Y., Chen H., Zhu Y.,** An in-line Mach-Zehnder interferometer using thin-core fiber for ammonia gas sensing with high sensitivity, Scientific reports. 7 (1) (2017) 44994.

4. **Romashkin A.V., Rozanov R.Yu., Lashkov A.V., Vishnevskiy A.S., Mitrofanova A.E., Levin D.D., Svetikov V.V.,** Change in the carbon nanotube thin layer refractive index after water and ammonia molecules adsorption, St. Petersburg State Polytechnical University Journal. Physics and Mathematics. 17 (3.1) (2024) 68–74.

5. **Rani S., Kumar M., Garg R., Sharma S., Kumar D.,** Amide functionalized graphene oxide thin films for hydrogen sulfide gas sensing applications, IEEE Sens. J. 16 (9) (2016) 2929.

6. **Avouris P., Martel R., Derycke V.,** Appenzeller J., Carbon nanotube transistors and logic circuits, Physica B: Condensed Matter. 323 (1–4) (2002) 6–14.

7. **Mi G., Horvath C., Van V.,** Silicon photonic dual-gas sensor for H_2 and CO_2 detection, Optics express. 25 (14) (2017) 16250–16259.

8. **Wang J., Zhang H., Chen S., Zhang Z., Wu G., Li X., Ding P., Tan C., Du Y., Geng Y., Li X., Tsang H. K., Cheng Z.,** A Silicon Microring Resonator for Refractive Index Carbon Dioxide Gas Sensing, ACS sensors. 10 (7) (2025) 4938–4944.

9. **Gelao G., Marani R., Perri A. G.,** A formula to determine energy band gap in semiconducting carbon nanotubes, ECS J. Solid State Sci. Technol. 8 (2) (2019) M19.

10. **Struchkov N.S., Romashkin A.V., Rabchinskii M.K., Saveliev S.D., Cherviakova P.D., Chumakov R.G., Nevolin V.K., Varezhnikov A.S., Emelianov A.V.,** Aminated reduced graphene oxide-carbon nanotube composite gas sensors for ammonia recognition, Sensors and Actuators B: Chemical. 417 (2024) 136088.

11. **Romashkin A.V., Lashkov A.V., Sysoev V.V., Struchkov N.S., Alexandrov E.V., Levin D.D.,** Energy-Efficient Chemiresistive Sensor Array Based on SWCNT Networks, WO_3 Nanochannels and SWCNT-Pt Heterojunctions for NH_3 Detection against the Background Humidity, Chemosensors. 10 (11) (2022) 476.

12. **Abdellah A., Abdelhalim A., Horn M., Scarpa G., Lugli P.,** Scalable spray deposition process for high-performance carbon nanotube gas sensors. IEEE Transactions on Nanotechnology. 12 (2) (2013) 174–181.

13. **Zhao J., Buldum A., Han J., Lu J.P.,** Gas molecule adsorption in carbon nanotubes and nanotube bundles, Nanotechnology. 13 (2) (2002) 195–200.

14. **Bogaerts W., De Heyn P., Van Vaerenbergh T., De Vos K., Kumar Selvaraja S., Claes T., Dumon P., Bienstman P., Van Thourhout D.,** Baets R., Silicon microring resonators, Laser & Photonics Reviews. 6 (1) (2012) 47–73.

THE AUTHORS

ROMASHKIN Alexey V.
romaleval@gmail.com
ORCID: 0000-0002-0101-6122

VISHNEVSKIY Alexey S.
alexeysw@mail.ru
ORCID: 0000-0002-4024-5411

ROZANOV Roman Yu.
roman-roz@yandex.ru
ORCID: 0000-0001-5063-1669

MITROFANOVA Anastasia E.
mitrofanova.ae@phystech.edu
ORCID: 0009-0004-5306-278X

STEBELKOV Artem N.
stebelkov@zntc.ru

NEPOMILUEVA Valeriya V.
valeria.nepomilueva@yandex.ru

LEVIN Denis D.
skaldd@yandex.ru
ORCID: 0000-0002-8414-6191

SVETIKOV Vladimir V.
svetikov@nsc.gpi.ru

NEVOLIN Vladimir K.
vkn@miee.ru

Received 13.08.2025. Approved after reviewing 18.08.2025. Accepted 20.08.2025.